NASA TECHNICAL NOTE

NASA TN D-4935

NASA TN D-4935

AN ESTIMATE OF THE SUPERSONIC FLOW FIELD ABOUT AN AXISYMMETRIC BODY WITH AN N WAVE PRESSURE TRACE

by Roger W. Luidens

Lewis Research Center

Cleveland, Ohio

NATIONAL AERONAUTICS AND SPACE ADMINISTRATION • WASHINGTON, D. C. • DECEMBER 1968

AN ESTIMATE OF THE SUPERSONIC FLOW FIELD ABOUT AN AXISYMMETRIC BODY WITH AN N WAVE PRESSURE TRACE

By Roger W. Luidens

Lewis Research Center
Cleveland, Ohio

NATIONAL AERONAUTICS AND SPACE ADMINISTRATION

For sale by the Clearinghouse for Federal Scientific and Technical Information
Springfield, Virginia 22151 – CFSTI price $3.00

ABSTRACT

Linearized flow assumptions and the conservation equations of mass, momentum, and energy are used to estimate the flow field at all distances from a body which produces an N wave pressure trace. The analytical results show good agreement with experimental results for cones and axisymmetric bodies with convex profiles. The influence of the shock wave entropy increase on the attenuation of the shock wave static pressure rise with distance from the body is illustrated.

AN ESTIMATE OF THE SUPERSONIC FLOW FIELD ABOUT AN AXISYMMETRIC BODY WITH AN N WAVE PRESSURE TRACE

by Roger W. Luidens

Lewis Research Center

SUMMARY

At the present time, the analysis of the sonic boom from overflying aircraft is important because of the efforts to reduce this disturbance by the proper selection of the airplane configuration and/or flight conditions. The analysis of sonic boom depends on the more fundamental and limited problem of describing the flow field about a body in a uniform flow, which is the subject of this report.

Linearized flow assumptions and the conservation equations of mass, momentum, and energy are used to estimate the flow field at all distances from an axisymmetric body of zero angle of attack that yields an N wave pressure trace. The analytical results were shown to be in good agreement with experimental results for cones and axisymmetric bodies with a convex profile.

The present analysis shows explicitly how the entropy increase across the initial shock wave contributes to the attenuation of the initial static pressure rise across the shock with increasing distance from the body. This effect occurs only implicitly with Fredrichs' hypothesis and in Whitham's far field analysis which assume adjacent isentropic flows with interposed shocks.

INTRODUCTION

At the present time, the analysis of the sonic boom from an overflying aircraft is important because of efforts to reduce this disturbance from the future supersonic transports by the design of the vehicle shape and/or by the selection of flight conditions. The analysis of the sonic boom depends on the more basic and more limited problem of describing the flow field about an axisymmetric body at zero angle of attack in a uniform flow field, and that is the subject of this report.

All the analyses cited in the following discussion deal with small disturbances in a uniform supersonic stream. The earliest analyses of flow about slender shapes (Hayes, 1947 (ref. 1) and Graham, et al., 1952 (summarized in ref. 2)) were concerned primarily with the lift and drag on these shapes. In these analyses, the assumption of irrotational and/or isentropic linearized flow was made. These analyses led to the area rules that evolved conceptually from considerations of the disturbances in the flow far from the body, Whitcomb, 1952 and 1953 (reported in refs. 3 and 4). While far field disturbances are predicated by the assumed isentropic flow, the disturbances of primary concern were those on the body which give rise to its lift and drag; and inaccuracies in the predictions of far field disturbances were of little consequence. This branch of analysis culminated in electronic computer programs, such as the one described in reference 5, for calculating the pressure forces on an airplane.

Unlike estimating the forces on a body, estimations of sonic boom require accurate determination of the disturbances far from the body. The first step in this direction was taken by Fredrichs' reference 6, for the two-dimensional supersonic flow about an airfoil. He hypothesized that a separate isentropic flow solution for the flow over the wing itself could be patched into the isentropic free stream flow by interposing shocks attached to the wing leading and trailing edges. The simultaneous assumption of isentropic flow and shock waves was admittedly conflicting.

Lighthill (ref. 7) examines Fredrichs' hypothesis in detail. For the shock shape predicted by Fredrichs, he found that the momentum loss in the flow associated with the entropy rise across the shock waves plus the momentum change in wave form between the leading and trailing shocks equaled the force on the body for all distances from the body. He concluded that Fredrichs' hypothesis was "watertight."

The hypothesis of Fredrichs, that of patching separate isentropic solutions by interposed shocks, was applied to the three-dimensional supersonic flow about an axisymmetric body by Whitham first in 1950 and updated in reference 8. Whitham's result is not in closed-form and is most conveniently applied using electronic computers as discussed in reference 9 for example. The accuracy of Whitham's analysis is supported by experimental results, reference 10 for example. References 11 and 12 are reviews of sonic boom analytical and experimental research and contain many more references.

The present analysis differs from the preceding ones in the following ways:

(1) The assumption of nonisentropic flow is made from the beginning.

(2) The analysis is made based on the conservation equations of mass, momentum, and energy, rather than Fredrichs' hypothesis.

(3) For a body which produces an N wave pressure trace, the present analysis yields an estimation of the flow field at all distances from the body. The analysis is approximately correct for general slender bodies at large distances. The approach of the present analysis should contribute to the understanding of shock wave attenuation and the closed form of the results will be a convenience for estimation purposes.

Closed form relations are developed for the general flow field about a body including the shock shape and initial static pressure rise. The analytical results are compared with experimental results, and typical flow field calculations are illustrated.

SYMBOLS

A	cross-sectional area of body normal to the x-direction $\mu = \mu_\infty$
A'	maximum cross sectional area of body
A_x	general projected area normal to the x-direction at station x
a	speed of sound
B	$\left[(\gamma + 1)/4\gamma\right](M^2/\beta)$
C_{D_p}	pressure-drag coefficient of forebody based on cross-sectional area at $\mu = \mu_\infty$
C_p	pressure coefficient, $(p - p_\infty)/(1/2)\gamma p M^2$
c	$\int_{\xi_{\mu=\mu_\infty}}^{\xi_m} u^2 d\xi \Big/ \int_0^{\xi_m} u^2 d\xi$
D_p	drag of forebody to station where $\mu = \mu_\infty$
E	$K_c \gamma M^2 \left[(A/l^2)\ (1/\beta)\right]^{1/2}$
K_c	$\sqrt{3C_{D_p}/4\pi c}$
K_s	body shape factor, $C_{D_p}/A/l^2)$
l	length of forebody from nose to station where $\mu = \mu_\infty$
l'	length of forebody from nose to maximum cross section
M	Mach number
P	total pressure
p	static pressure
Δp	static pressure rise, above ambient
U	free-stream velocity in x-direction

U_v	velocity for isentropic expansion to zero pressure
u, v	perturbation velocities in x- and r-direction, respectively
x, r, θ	cylindrical coordinates (see fig. 1)
γ	ratio of specific heats
ζ	ξ_m minus l, see fig. 3
μ	angle between local Mach wave or shock wave and free-stream direction
μ_M	angle between local Mach wave and local-stream direction
μ_∞	angle between free-stream Mach wave and free-stream direction
ξ	coordinate in minus x-direction measured from reference Mach wave originating from position on the body where $\mu = \mu_\infty$
ξ_m	sound wave length, length between initial static pressure rise and position where $\mu = \mu_\infty$
ρ	air density

Subscripts

e	entropy component
m	behind leading shock or at body nose
max	maximum value
p	body pressure drag
r	in r–direction
t	body trailing edge or trailing shock
w	sound wave component
x	in x–direction, or at station x
∞	free-stream value
1	radius of body
2	outer radius of control surface

ANALYSIS

The Momentum Equation and Basic Assumptions

The present analysis is based on the momentum theorem which states, for steady flow, that the time rate of change of momentum through the surfaces at a fixed control volume is equal to the net force acting on the fluid (ref. 13). The coordinate system used for the analysis is shown in figure 1. It is a conventional cylindrical x, r, θ coordinate system with the free-stream velocity U in the x-direction; u and v are perturbation velocities in the x- and r–direction, respectively. The surfaces of the control volume to which the momentum theorem will be applied are those of the circumscribing cylinder shown in figure 1.

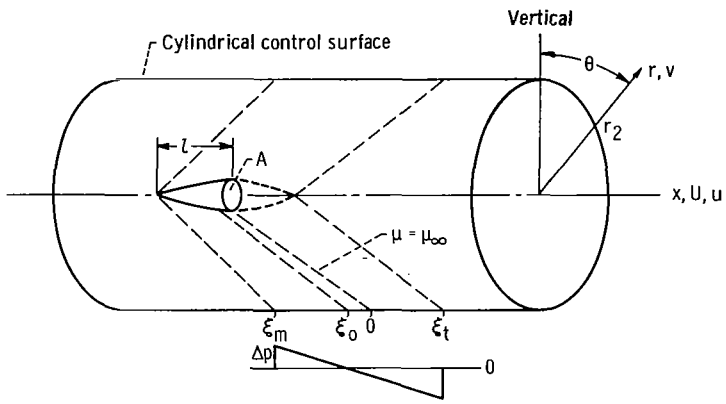

Figure 1. - Coordinate system and control volume.

The cylinder is selected so that the sides are parallel to the free-stream direction, the upstream end is in the free-stream where the static pressure is p_∞, and the downstream end is located sufficiently far downstream so the static pressure has again returned to p_∞. The integral of the pressure forces on the control surface

$$\int_{\substack{\text{control}\\ \text{surface}}} (p - p_\infty) dA_x$$

is thus zero. The only pressure force on the fluid and in the x-direction is the integral of the pressures on the body

$$\int_{body} (p - p_\infty) dA_x$$

which is the body pressure drag, D_p. Friction forces are not considered in this analysis, so the body pressure drag is the only force acting on the fluid.

The rate of change of momentum in the x-direction is the mass flow rate times the change in velocity in the x-direction. The body causing the momentum change is taken as axisymmetric (and at zero lift) and the fluid properties are taken as uniform (and hence axisymmetric), so the problem is axisymmetric. The mass flux through an elemental cylinder of the side of the control surface due to the velocity component normal to that surface is $2\pi r_2 \rho v \, dx$, and the velocity component in the x-direction of that fluid element is $(U + u)$ so that the velocity change from the free-stream velocity U is u. A mass flux through the sides of the control cylinder exists only between ξ_m and ξ_t. At other regions the streamlines and the sides of the control cylinder coincide.

Through the trailing end of the control cylinder, the mass flux per cylindrical element is $2\pi r \rho (U + u) dr$, and the change in velocity from the free-stream value in the x-direction is u.

The present analysis considers only small changes in velocity from the free-stream value, so that in estimating the mass flux through the walls of the control cylinder, changes in the fluid density ρ may be neglected, and u may be neglected compared with with U. Also, only a forebody, as indicated by the solid lines in figure 1, is considered to permit only the leading shock from the body. The forebody generates the forepart of the N wave pressure trace on the side of the control cylinder. The forebody is defined to terminate where the wave angle leaving the body is equal to the free stream Mach wave angle. Downstream of this wave the flow is assumed to return to the x axis and the free stream direction isentropically. (An alternative assumption that the forebody and afterbody generate the same pressure drag and shock losses would yield the same end result.) Then, equating the net force on the fluid (the pressure drag on the body D_p) to the rate of change of momentum yields

$$D_p = - 2\pi r_2 \rho \int_{\xi_{\mu=\mu_\infty}}^{\xi_m} vu \, d\xi - 2\pi \rho U \int_0^{r_2} ur \, dr \qquad (1a)$$

The pressure drag on the body is seen to give rise to two drag components in the flow field. The first term on the right-hand side of equation (1a) will be called the "sound wave component", because it is the component that carries the sonic boom, and designated D_w. The second component will be called the "entropy component", and designated D_e, because it will be calculated from the increase in entropy (loss in total

pressure) across the shock waves in the system. (The friction drag would also appear as a defect in momentum in the downstream plane but, as mentioned before, this is not considered here. Also, to help clarify the terminology being used, note that the sum of the two terms on the right-hand side of equation (1a) is generally referred to as the shock wave drag or simply the body wave drag.) The selection of the cylindrical control surface shown in figure 1 is convenient because the sound wave drag and entropy drag cause disturbances in clearly distinct regions; that is, respectively, on the sides and end of the control cylinder.

In abbreviated form, equation (1a) can be written as

$$D_p = D_w + D_e \tag{1b}$$

that is, the sum of the sound wave and entropy drags must equal the pressure drag on the body. One part of the problem dealt with in this paper is how the sound wave drag and entropy drag components are divided as a function of the distance r_2 from the body. Qualitatively, for the cylindrical wall of the control surface very near the body, r_2 small, the drag in the flow is predominantly in the form of sound wave drag. As the distance of the cylindrical wall from the body increases, r_2 increasing, more of the drag must appear as entropy drag due to the total pressure losses across the leading shock wave. As r_2 approaches infinity, it is expected that all of the drag appears as entropy drag and the sound wave drag has decayed to zero.

Also, for an axisymmetric body, attenuation of the initial pressure rise in the sound wave with increasing distance from a body is associated with three effects, all of which are interrelated:

(1) The cylindrical attenuation that would exist even if the leading and trailing waves were parallel and isentropic.

(2) The attenuation due to a divergence of the leading shock and the downstream Mach waves

(3) The attenuation in the sound wave drag due to a conversion of some of the body pressure drag to entropy drag.

The sound wave component of the drag will be analyzed by applying the linear theory relation between the perturbation velocities u and v along any given stream tube, that is

$$v = -\beta u \tag{2a}$$

where

$$\beta = \sqrt{M^2 - 1} \tag{2b}$$

The linearized relation between static pressure change from the free-stream value $\Delta p \equiv p - p_\infty$ and the velocity change u is

$$\Delta p = \rho U u \tag{3}$$

A discussion of linearized theory may be found in references 1, 2, 8, and 13 for examples.

The entropy component of the drag will be analyzed knowing that: (1) the total energy along a stream tube remains constant; (2) the "available energy", as measured by the stream entropy or total pressure, is a characteristic of each individual stream tube; and (3) the flow has returned to the free stream static pressure at the downstream surface of the control volume. The velocity change u at the trailing end of the control cylinder then depends on the total pressure losses incurred upstream along a given stream tube.

The problem has now been set up in general terms. To determine the initial shock pressure rise and shock shape, separate consideration is next given to the sound wave and entropy drags and their relation to the leading shock shape.

Sound Wave Drag

This part of the analysis will lead to relations between the sound wave drag and the static pressure rise across the shock which, in turn, is a function of the leading shock shape.

Relation of sound wave drag to shock static pressure rise. - Using equation (2a), the sound wave drag may be written from equations (1a) and (1b) as follows

$$D_w = 2\pi r_2 \rho\beta \int_{\xi_{\mu=\mu_\infty}}^{\xi_m} u^2 \, d\xi \tag{4}$$

Conceptually, only the fore part of the body is being considered. To evaluate the integral in equation (4), it is assumed that the pressure signature of the sound wave at all radii r is the fore part of an N wave, that is, that $\Delta p/p$ varies linearly with ξ as shown in figure 2(a). This agrees with the analysis of reference 8 and with the experimental results of reference 10, both for the far field. This, strictly speaking, limits the analysis to bodies that produce a pressure trace that is the fore part of an N wave at all distances.

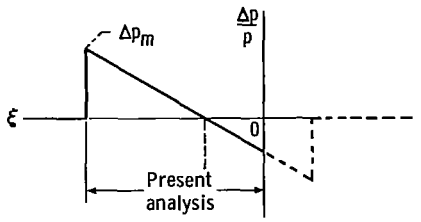

(a) Assumed N-wave static pressure signature.

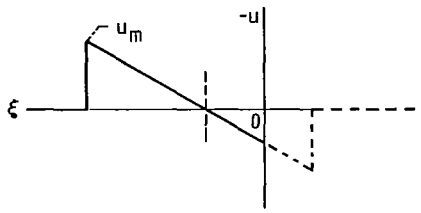

(b) Perturbation velocity u_w.

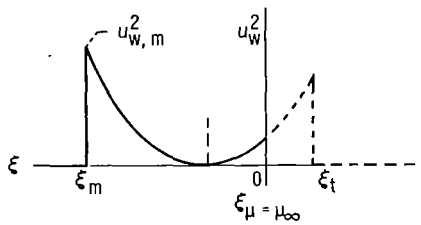

(c) Perturbation velocity squared u_w^2.

Figure 2. - Assumed disturbances in flow field on sides of control cylinder.

Then, by equation (3), u must also vary linearly with ξ, as shown in figure 2(b). As shown in figure 2(c), the variation of u^2 with ξ has a parabolic shape. From the geometry of figure 2(c), the integral in equation (4) can then be written in terms of u_m^2 as

$$\int_{\xi_{\mu=\mu_\infty}}^{\xi_m} u^2 \, d\xi = c \int_0^{\xi_m} u^2 \, d\xi = \frac{1}{3} c u_m^2 \xi_m \tag{5}$$

where the numerical value of c is approximately unity and is assumed so later. With the assumption of the form of u, the maximum over-pressure in the signature Δp_m in figure 2(a), depends only on the pressure drag of the body. Using the definition of the drag coefficient, the sound wave drag may also be written as

$$D_w = \frac{1}{2} C_{D_p} \rho U^2 A \frac{D_w}{D_p} \tag{6}$$

With equations (5) and (6) substituted in equation (4), it may be solved for u_m. The static pressure rise at leading shock (the front of the sound wave) may then be obtained from equation (3).

$$\frac{\Delta p_m}{\rho} = K_c U^2 \sqrt{\frac{\frac{A}{l^2}\frac{D_w}{D_p}}{\beta \frac{\xi_m}{l}\frac{r_2}{l}}} \tag{7a}$$

where

$$K_c = \sqrt{\frac{3C_{D_p}}{4\pi c}} \tag{7b}$$

Because the free-stream flow field Mach number will usually be specified, it is convenient to write the above result in terms of the Mach number, M = U/a. This is most conveniently done by recalling that the dynamic pressure q can be written in either of the following forms

$$q = \frac{1}{2}\rho U^2 = \frac{1}{2}\gamma p M^2 \tag{8}$$

Then using equation (8), equation (7a) may be written in terms of Mach number and ambient pressure as

$$\frac{\Delta p_m}{p} = K_c \gamma M^2 \sqrt{\frac{\frac{A}{l^2}\frac{D_w}{D_p}}{\beta \frac{\xi_m}{l}\frac{r_2}{l}}} \tag{9}$$

For the present study, if Δp_m, the initial static pressure rise in the sound wave, and the wave length ξ_m are known as a function of r_2/l, the problem is essentially solved. Unknown in equation (9) are ξ_m/l and D_w/D_p both of which are a function of r_2/l and these will be evaluated. The required functions depend on the shape of the leading shock which in turn depends on $\Delta p_m/p$ and this is discussed next.

Relation of shock static pressure rise to shock shape. - The air flowing around the slender body is first compressed as the body cross sectional area increases and then expands as the cross-sectional area approaches a cylindrical section. At some point along the body, it is hypothesized that a "reference Mach wave", having an angle the same as the free-stream Mach wave, μ_∞, leaves the body and extends outward (presumably as a straight line) to infinity; see figure 3. The Mach number and flow direction on the body where the reference Mach wave originates are not necessarily the free-stream values. The "forebody" referred to in the previous section is the body ahead of the point on the body from which the "reference Mach wave" leaves. The overpressure due to the forebody is, for the most part, positive as shown in figure 2(a), and this is the region of flow discussed in the present analysis. The leading shock shape is defined by the distance ξ_m that it lies ahead of the reference Mach wave. This distance consists of two parts, the length of the forebody, l, plus the remaining distance ζ (see fig. 3). The general relation for ζ may be written as

$$\zeta(r_2) = \int_0^{r_2} \frac{d\zeta}{dr}\, dr \tag{10}$$

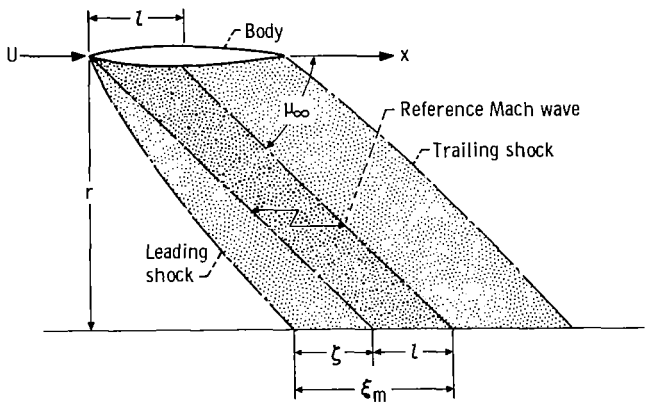

Figure 3. - Geometry for shock wave displacement analysis.

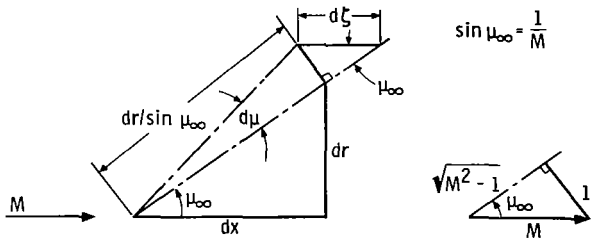

Figure 4. - Displacement of shock wave from Mach wave.

To integrate equation (10), the shock intensity is assumed to be weak consistent with linearized theory so that the deviation of the shock angle from the Mach angle, $\Delta\mu \equiv \mu - \mu_\infty$, is small. Then from the geometry of figure 4, the differential $d\xi/dr$ may be written

$$\frac{d\xi}{dr} = \frac{ds}{dr}\left(\frac{ds}{d\xi}\right)^{-1} = \frac{d\mu}{\sin^2\mu_o} = M^2\left(\frac{d\mu}{\frac{dp_m}{p}}\right)\frac{dp_m}{p} \tag{11}$$

The term $d\mu/(dp_m/p)$ may be found by differentiating equation (155) of reference 14 for the relation between μ and p_m/p.

$$\frac{d\mu}{\frac{dp_m}{p}} = \frac{\gamma+1}{4\gamma}\frac{1}{\beta} \tag{12}$$

Using equations (10), (11), and (12) and the difference form $\Delta p/p$ for dp/p consistent with equation (9), the equation for ξ_m is

$$\frac{\xi_m(r_2)}{l} = 1 + \frac{\gamma+1}{4\gamma}\frac{M^2}{\beta}\int_0^{r_2/l}\frac{\Delta p_m}{p}\,d\left(\frac{r}{l}\right) \tag{13}$$

Equations (9) and (13) are a pair of equations that are to be solved for the pressure rise Δp_m. In these equations, a number of terms are constants. The ratio of specific heats, γ, is taken as a constant. The terms, M, β, and p are specified free-stream airflow conditions and the terms l, A, and K_c are specified body shape and aerodynamic characteristics. The remaining terms Δp_m, ξ_m, D_w/D_p are dependent variables; r_2 is considered the independent variable. Equations (9) and (13) can be combined to eliminate $\Delta p_m/p$ by first differentiating equation (13), and this gives equation (14). In equation (14), the variables have been separated; and the constants in equations (9) and (13) have been lumped together.

$$\left(\frac{\xi_m}{l}\right)^{1/2} d\left(\frac{\xi_m}{l}\right) = BE\left(\frac{D_w}{D_p}\right)^{1/2}\left(\frac{r}{l}\right)^{-1/2} d\left(\frac{r}{l}\right) \tag{14a}$$

where the constants from equation 9 are

$$E = K_c \gamma M^2 \left(\frac{A}{l^2} \frac{1}{\beta} \right)^{1/2} \tag{14b}$$

and from equation (13) are

$$B = \frac{\gamma + 1}{4\gamma} \frac{M^2}{\beta} \tag{14c}$$

In equation (14a), the sound wave drag fraction, D_w/D_p, must decrease with increasing distance ratio, r_2/l, due to the cumulative increase in entropy related to the increase in mass flow through the downstream end of the control cylinder with increasing r_2/l. The sound wave length ratio, ξ_m/l also increases with increasing r_2/l. A mathematical form for the wave drag fraction consistent with these observations and with the form of equation (14a); that is, D_w/D_p taken as a power of (ξ_m/l) is

$$\frac{D_w}{D_p} = \left(\frac{\xi_m}{l} \right)^{-n} \tag{15}$$

where the exponent n is a positive number yet to be determined. Substituting this relation in equation (14a) and carrying out the integration gives

$$\frac{\xi_m}{l} = \left[1 + BE(n+3) \left(\frac{r_2}{l} \right)^{1/2} \right]^{2/(n+3)} \tag{16}$$

Equation (16) describes the sound wave length ξ_m and, hence, the leading shock shape in terms of r_2/l and the unknown exponent, n.

These results (eqs. (15) and (16)) may be substituted in equation (9) to give the initial pressure rise in the sound wave also in terms of n as

$$\frac{\Delta p_m}{p} = E \left(\frac{\xi_m}{l} \right)^{-(n+1)/2} \left(\frac{r_2}{l} \right)^{-1/2} = E \left[1 + BE(n+3) \left(\frac{r_2}{l} \right)^{1/2} \right]^{-(n+1)/(n+3)} \left(\frac{r_2}{l} \right)^{-1/2} \tag{17}$$

The determination of a value for n depends on the analysis of the entropy drag which is discussed next.

Entropy Drag

This discussion parallels that of the wave drag.

Relation of entropy drag to shock static pressure rise and shape. - The entropy drag is most conveniently discussed by forming the ratio of the entropy drag to the body pressure drag. This may be done in drag coefficient form, recalling that, in general, $C_D = D/(1/2)\rho U^2 A$. From the term for the entropy drag in equation (1), the second term on the right-hand side, we can write

$$\frac{D_e}{D_p} = \frac{C_{D_e}}{C_{D_p}} = \frac{-4\pi}{C_{D_p}\frac{A}{l^2}} \int_0^{r_2/l} \frac{u}{U}\frac{r}{l}\, d\left(\frac{r}{l}\right) \tag{18}$$

To evaluate the integral in this equation, we need to know u/U as a function of r/l. Equation (17) (with $r_2/l = r/l$) gives $\Delta p_m/p$ as a function of r/l, so if u/U can be evaluated in terms of $\Delta p_m/p$, we will have the required relation. The conditions for evaluating u/U at the downstream end of the control cylinder were stated earlier and are reviewed here: (1) the total energy along the stream tube remains constant; (2) the "available energy" as measured by the stream entropy or total pressure, is a characteristic of each individual stream tube; and (3) the flow has returned to the free-stream pressure at the downstream end of the control surface.

The following are the mathematical manipulations required to obtain the desired relation between u/U and $\Delta p_m/p$. Equation (71) of reference 14 is an appropriate one relating the velocity of the downstream plane to the stream total pressure. In the terminology of this report, it is

$$\frac{p}{P} = \left[1 - \left(\frac{U}{U_v}\right)^2\right]^{\gamma/(\gamma-1)} \tag{19}$$

U_v is the velocity for expansion to zero pressure and depends only on the total energy in the stream, which is a constant, and not on the total pressure, P. Thus, U_v is a constant. The static pressure, p, while it has undergone an excursion from the free-stream value between the leading shock and the trailing wave from the body, has returned to the free-stream value in the vertical plane downstream of the body being considered here,

and is thus a constant at the free-stream value. P and U are then the only variables. Equation (19) may be differentiated to yield (Note that dU = u.)

$$\frac{dP}{P} = \frac{2\gamma}{\gamma - 1}\left[1 - \left(\frac{U}{U_v}\right)^2\right]^{-1}\left(\frac{U}{U_v}\right)^2 \frac{u}{U} \tag{20}$$

Equation (76) of reference 14 gives (Note: the term $(\gamma + 1)$ in eq. (76) of ref. 14 should read $(\gamma - 1)$.)

$$M^2 = \frac{2}{\gamma - 1}\left[1 - \left(\frac{U}{U_v}\right)^2\right]^{-1}\left(\frac{U}{U_v}\right)^2 \tag{21}$$

so, equation (20) may be written

$$\frac{u}{U} = \frac{1}{\gamma M^2}\frac{dP}{P} \tag{22}$$

This gives the relation between the velocity at the downstream end of the control cylinder, and the total pressure loss, dP, along the streamline upstream of the integration plane.

Equation (113) of reference 14 gives a series relating the total pressure ratio across a weak shock wave to the static pressure rise across that shock. For a sufficiently weak wave, the first term of that series is an adequate approximation; it is

$$\frac{P_m}{P_\infty} = 1 - \left(\frac{\gamma + 1}{12\gamma^2}\right)\left(\frac{p_m}{p_\infty} - 1\right)^3 \tag{23}$$

where station ∞ is ahead of the shock, and station m after the shock. Because this relation holds only for p_m/p_∞ close to unity, it can be appropriately written

$$\frac{dP}{P} = -\frac{\gamma + 1}{12\gamma^2}\left(\frac{dp}{p}\right)^3 \tag{24}$$

This relation may be combined with equation (22) to give

$$\frac{u}{U} = -\frac{\gamma + 1}{12\gamma^3 M^2}\left(\frac{dp_m}{p}\right)^3 \tag{25}$$

This is the sought after relation between u/U and the static pressure rise across the leading shock wave. The integration of equation (18) can now be carried out by substituting equation (17) in equation (25), and equation (25) in equation (18). The result for the ratio of entropy to body pressure drag is

$$\frac{D_e}{D_p} = \frac{1}{cn}\left[1 - \left(\frac{\xi_m}{l}\right)^{-n}\right] \tag{26}$$

This is still in terms of the unknown exponent n.

Determination of shock shape exponent n. - From equation (1b), which relates the sound wave and entropy drags, and equation (15) for the assumed algebraic form for the entropy drag, we can write

$$\frac{D_e}{D_p} = 1 - \frac{D_w}{D_p} = 1 - \left(\frac{\xi}{l}\right)^{-n} \tag{27}$$

By comparing equations (26) and (27), it can be seen that the condition that both equations be true is that the coefficient of equation (26) be unity; that is, that cn = 1. This happily simple result is due in part to the choice of the form of equation (15). Recall that earlier it was indicated that c was nearly unity; the approximation is made here that c = 1.0, so n = 1.0, and the problem is solved within the assumptions that have been made. The approximation c = 1.0 corresponds to taking the positions on the pressure trace where $\mu = \mu_\infty$ and $\Delta p = 0$ as coincident, see figure 2. This is a good approximation at some distance from the body, but only a fair approximation very close to the body.

Summary of Equations

The preceding results are summarized here. For the sound wave flow field, equations (16), (17), (3), (2a), and (15), respectively give

$$\frac{\xi_m}{l} = \sqrt{1 + \sqrt{\frac{3K_s}{4\pi c}} \cdot \frac{(\gamma + 1)M^4}{\beta^{3/2}} \cdot \left(\frac{A}{l^2}\right) \cdot \left(\frac{r_2}{l}\right)^{1/2}} \tag{28}$$

$$\frac{\Delta p_m}{p} = \frac{\sqrt{\frac{3K_s}{4\pi c}}\,\gamma M^2\left(\frac{A}{l^2}\right)}{\sqrt{\beta\frac{r_2}{l}\left(\frac{\xi_m}{l}\right)^2}} \tag{29}$$

$$\left(\frac{u}{U}\right)_{wm} = \frac{1}{\gamma M^2}\,\frac{\Delta p_m}{p} \tag{30}$$

$$\left(\frac{v}{U}\right)_{wm} = -\beta\frac{u_{wm}}{U} \tag{31}$$

$$\frac{D_w}{D_p} = \left(\frac{\xi_m}{l}\right)^{-1} \tag{32}$$

For the entropy flow field, equations (25) and (27), respectively, give

$$\left(\frac{u}{U}\right)_e = -\frac{\gamma + 1}{12\gamma^3 M^2}\left(\frac{\Delta p_m}{p}\right)^3 \tag{33}$$

where $\Delta p_m/p$ is given by equation (29) and

$$\frac{D_e}{D_p}\left(\frac{r_2}{l}\right) = 1 - \frac{D_w}{D_p}\left(\frac{r_2}{l}\right) \tag{34}$$

Approximate relations. - Equations (28) and (29) can be approximated for the near and far field. The near field is defined here as, when the ξ_m/l can be approximated by unity. This eliminates the need for equation (28) and simplies equation (29). For this case, Δp_m is proportional to (A/l^2) and inversely related to the square root of r_2/l.

The far field is defined here as, when in the equation (28), the term unity can be neglected to a good approximation. In this case, equation (29) for the static pressure

rise becomes

$$\frac{\Delta p_m}{p} = \left(\frac{3K_s}{4\pi c}\right)^{1/4} \frac{\gamma}{(\gamma+1)^{1/2}} \beta^{1/4} \left(\frac{A}{l^2}\right)^{1/2} \left(\frac{r_2}{l}\right)^{-3/4} \tag{35}$$

Now Δp_m is proportional to the square root of A/l^2 and inversely with r_2/l to the 3/4 power. Equation (35) is the expression usually given for the far-field static pressure rise except for the form of the first term. While these approximations may be made, the present analytical expressions are sufficiently simple that the approximations are not needed.

Application of the results. - In order to apply the preceding equations, several terms must be known; K_s, and the location on the body for the origin of the reference Mach wave.

The term $K_s \equiv C_{D_p}(A/l)$ is in general a function of: Mach number, A/l^2, and body profile shape. K_s has been evaluated for cones using the information in Chart 6 of reference 14 and the results are presented in figure 5. For a cone, K_s and A_x/x^2 are constant along the length of the body. This is not true for other profile shapes. An analysis to determine the body profile with minimum drag, presented in Truitt, ref-

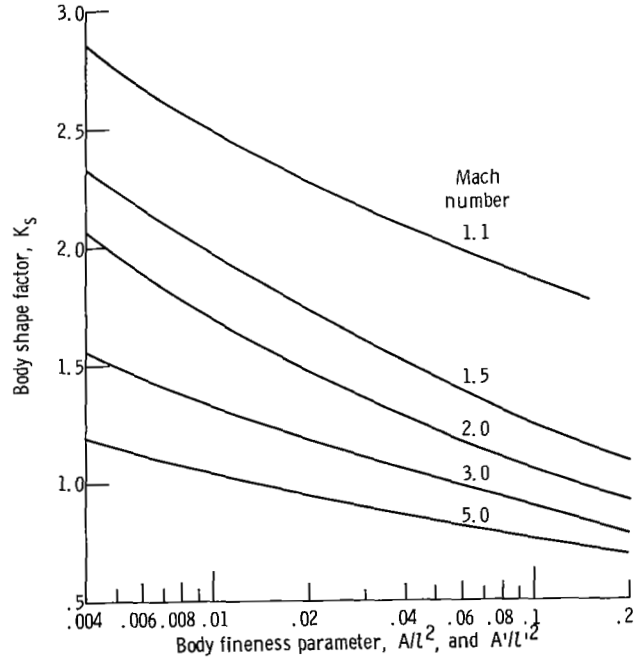

Figure 5. - Body shape factors for cones.

ence 5, suggests that such a profile has a K_s of 0.67 that of a cone with the same A'/l'^2. In applying the results to nonconical shapes, A'/l'^2 is used for A/l^2.

For a body with a convex profile, it can be estimated analytically that the reference free-stream Mach wave leaves at about $0.86l'$. A similar value is suggested for both a minimum drag profile and for cones by the experimental results of reference 10. Because it is convenient in applying the results to have them in terms of the length to the maximum cross-sectional area, equations (28) and (29) are rewritten below for $l = 0.85\,l'$, and A/l^2 taken as A'/l'^2.

$$\frac{\xi_m}{l'} = 0.85\sqrt{1 + \left(\frac{3K_s}{4\pi}\right)^{1/2} \frac{(\gamma+1)M^4}{\beta^{3/2}} \left(\frac{A'}{l'^2}\right)\left(\frac{r_2}{0.85l'}\right)^{1/2}} \tag{36}$$

$$\frac{\Delta p_m}{p} = \frac{\left(\frac{3K_s}{4\pi}\right)^{1/2} \gamma M^2 \left(\frac{A'}{l'^2}\right)}{\sqrt{\beta \frac{r_2}{0.85l'}\left(\frac{\xi_m}{0.85l'}\right)^2}} \tag{37}$$

Also, at some distance from the body, the sound wave length, ξ_m, is to a good approximation the distance between the initial static pressure rise and the position where $\Delta p = 0$.

DISCUSSION

Here a comparison with experimental results is given, and the results of typical flow field calculations are illustrated.

Comparison with Experimental Results

Reference 10 gives experimental data presented in figure 6 for the pressure field about a number of bodies of revolution, at Mach numbers of 1.26, 1.41, and 2.01. The bodies used for comparison with the analytical results are given in table I. They yield nearly half N-wave shapes at the distances considered. From these data, the peak pressure rise, which is not always the initial pressure rise for the conical bodies, and the sound wave length can be determined.

Also presented in figure 6 for comparison with experimental results are the analytical results of equations (36) and (37). Figure 6(a) presents the dimensionless sound wave length, ξ_m/l', versus the dimensionless distance from the body r_2/l'. The data for model 1 are very nearly the same as those for model 7 and, hence, not shown.

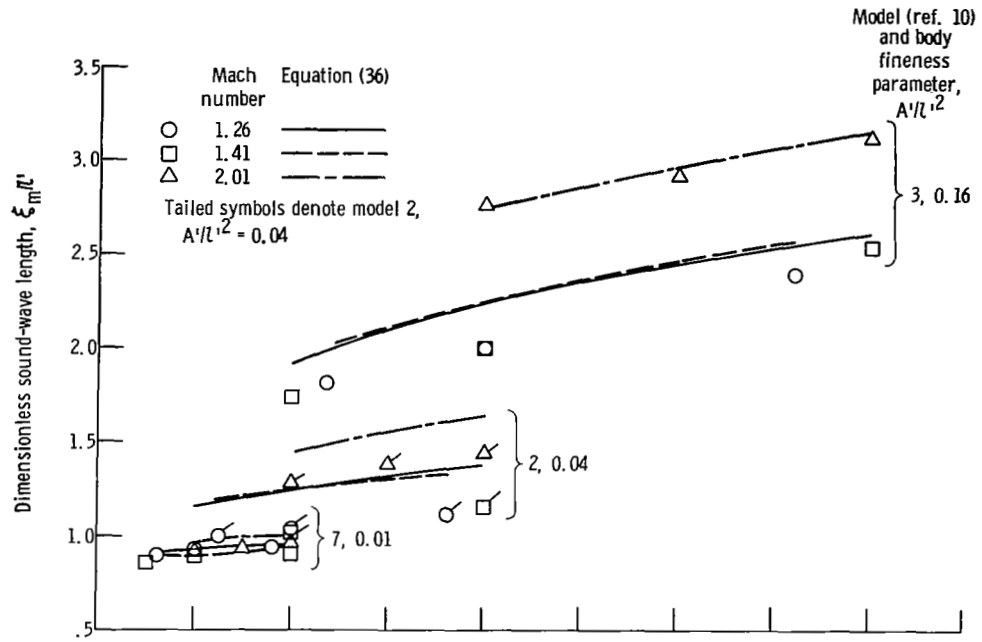

(a) Sound-wave length.

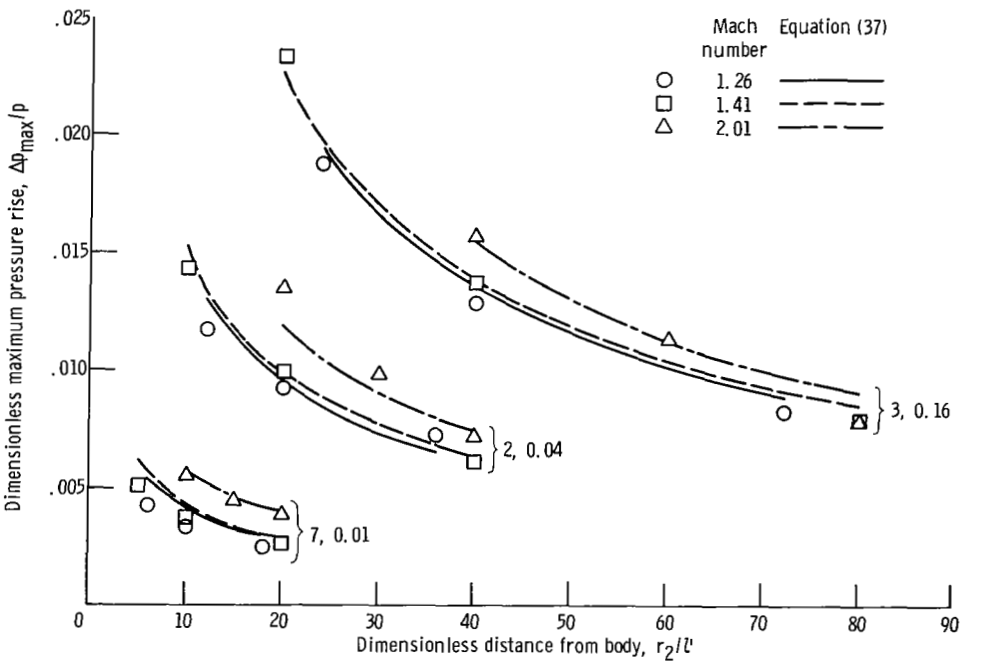

(b) Peak pressure rise.

Figure 6. - Comparison of analytical and experimental results.

TABLE I. - BODY SHAPES

Body profile	Body fineness parameter A'/l'^2	Model (ref. 10)
Conical	0.01	1
Conical	.04	2
Conical	.16	3
Minimum drag	.01	7

The data for model 7 is near field data because ξ_m/l' is approximately unity. The remaining data is mid-field data because ξ_m/l' is of the same order as unity. In all cases, the agreement between the trends in the theory and data are correct. The agreement in absolute level is fairly good. This is attributable in part to the selection of the position from which the reference Mach wave leaves as $0.85\ l'$. Models 2 and 3 are cones, and for cones the near field sound wave shape is quite different from the half N wave assumed in the analysis. For a cone the peak pressure in the near field occurs some distance behind the initial shock, and hence the local shock angle, μ, and hence ξ_m would be expected to be less than would occur for an N wave. The comparison between the experimental and analytical results show this tendency.

Figure 6(b) presents the dimensionless maximum static-pressure rise in a similar plot. The experimental and analytical results are in surprisingly good agreement. The agreement is good even for the cones where as noted in the preceding paragraph the peak pressure occurs some distance downstream of the shock wave, and the estimation of the wave length is only fairly good.

The preceding results were for the near and mid-field. The analytical expressions reduce to the presently accepted analytical form in the far field.

It is concluded that for bodies of revolution with a conical or convex profile that the sound wave length and the maximum static-pressure rise can be approximated at all distances from the body by the simple closed form expression resulting from the present analysis.

Example Flow Field Results

A unique feature of the present analysis is that it determines the distribution in the flow of the sound wave drag and entropy drag components of the pressure drag. Also, all the flow field perturbation components may be estimated. Examples of such results are presented in figures 7 and 8. For these illustrative calculations, it has been assumed that

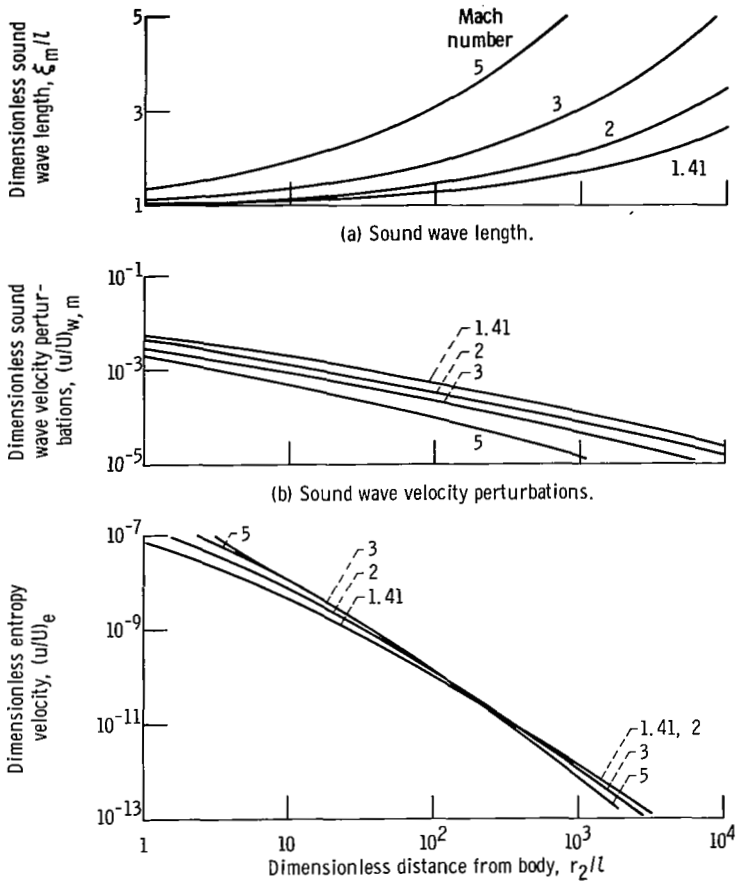

(a) Sound wave length.

(b) Sound wave velocity perturbations.

(c) Entropy velocity perturbation.

Figure 7. - Flow field about axisymmetric body with body parameter $(3K_s/4\pi)^{1/2} \times A/l^2 = 0.02$.

$$\sqrt{\frac{3K_s}{4\pi}}\,\frac{A}{l^2} = 0.02$$

These results will be discussed primarily from the point of view of the effect of distance from the body. To obtain the total effect of Mach number, the effect of Mach number on K_s, as illustrated in figure 5 (p. 18), would have to be accounted for. The effect of K_s in the far field is not large because, for example, it occurs to the one quarter power in the pressure rise (eq. (35)).

Figure 7(a) shows that the sound wave length ξ_m/l, equation (28), increases with distance from the body, r_2/l; and that for a given value of r_2/l, ξ_m/l increases with increasing Mach number. For the sake only of selecting some numerical values for discussion, it is noted that a supersonic transport may cruise at Mach number 3.0, may have a half-fuselage length, l, of 150 feet (45.7 m), and may fly at an altitude of 60 000 feet (18 210 m). This would give a value of r_2/l of 400. At this value of r_2/l

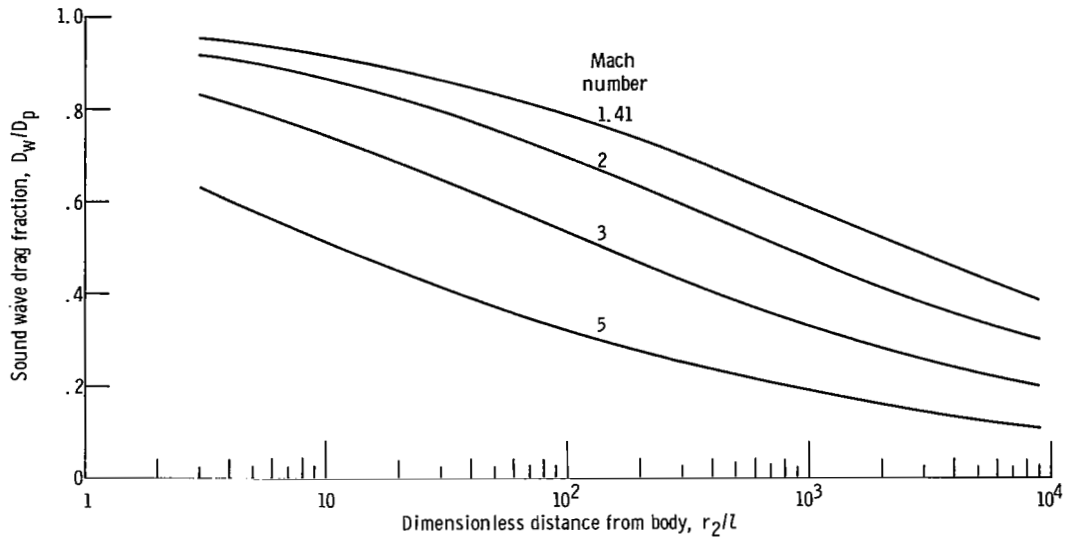

Figure 8. - Distribution of sound wave and entropy drag in flow field for axisymmetric body, with body parameter $(3K_s/4\pi)^{1/2}A/l^2 = 0.02$.

and at $M = 3.0$, ξ_m/l has a value of 2.5 compared with 1.0 at the body, $r_2/l = 0$. For the present analysis to apply for a sonic boom analysis, account would have to be taken of the density variation that exists in the Earth's atmosphere with distance from the body and, of course, of wing volume and lift effects. These effects are discussed in references 11 and 12, for example.

The value of $-(u/U)_{wm}$, equation (30), a sound wave component of the flow, is shown in figure 7(b). Recall that $\beta(v/U)_{wm} = -(u/U)_{wm}$, equation (31). These values decrease by orders of magnitude with increasing distance and also decrease with increasing Mach number. The values of the entropy component of the flow, $(u/U)_e$, equation (33), are shown in figure 7(c). These values also decrease by orders of magnitude with increasing r_2/l, but the effect of increasing Mach number varies with r_2/l.

The values of $(u/U)_e$ are many orders of magnitude smaller than the values of $(u/U)_{wm}$; for example, at $r_2/l = 400$, $(u/U)_w \approx 10^{-4}$, while $(u/U)_e \approx 10^{-11}$, seven orders of magnitude smaller. In spite of this, u_e can be of comparable importance to u_w in its contribution to the drag at distances far from the body because the mass flow parameter associated with u_e is $\rho\,(U/U)\pi(r_2/l)^2$ compared with $\rho(v/U)2\pi(r_2/l)$ associated with u_w, or about six orders of magnitude greater at $r_2/l = 400$.

The relative contribution to the drag of u_w and u_e is indicated by the fraction of the body pressure drag that appears in the form of sound wave drag and entropy drag, equations (32) and (34). This is shown in figure 8. Close to the body, $r_2/l \approx 1.0$, most (about 85 percent at $M = 3.0$) of the body pressure drag is in the form of sound wave drag. The remaining drag appears in the form of entropy drag. At $r_2/l = 400$ and $M = 3.0$,

however, only 40 percent of the pressure drag appears in sound wave drag form; and the remaining 60 percent in the entropy drag form. For a given value of r_2/l the fraction of the pressure drag in sound wave form decreases with increasing Mach number. With regard to the sonic boom, recall that only the sound wave form of the drag contributes to it.

The continuous degradation of the pressure drag into entropy drag with increasing distance from the body appears explicitly in the present analysis. This same process exists implicitly when Fredrichs' hypothesis is made as is done in Whitham's far field analysis, reference 8.

CONCLUDING REMARKS

Linearized flow assumptions and the conservation equations of mass, momentum, and energy were used to estimate the flow field about an axisymmetric body at zero angle of attack which produces a sound wave pressure trace. The results apply at all distances from the body.

The analytical results showed good agreement with experimental results for cones and axisymmetric bodies with convex profiles.

The present analysis shows explicitly how the entropy increase in the flow field shock waves contributes to the attenuation of the shock wave initial static pressure rise with increasing distance from the body. This effect occurs implicitly in Whitham's far field analysis which assumes isentropic flows with interposed shock waves.

The method of analysis in its present form does not give the detailed effect of body profile and the corresponding details in the pressure signature that Whitham's near field approach does. However it should contribute to the understanding of the flow phenomenon involved in the relation between shock attenuation with distance and shock losses. The simplicity of the present result will be a convenience for estimation purposes.

It is believed that the present approach can be extended to include the effects of atmospheric pressure and temperature gradients and perhaps a wave-shape that varies with distance from the body. This may contribute to achieving a simple closed form relation for estimating airplane sonic boom.

Lewis Research Center,
National Aeronautics and Space Administration,
Cleveland, Ohio, July 30, 1968,
126-15-02-02-22.

REFERENCES

1. Hayes, Wallace D.: Linearized Supersonic Flow. Rep. AL-222, North American Aviation, Inc., June 18, 1947.

2. Graham, E. W.; Lagerstrom, P. A.; Licher, R. M ; and Beane, B. J.: A Theoretical Investigation of the Drag of Generalized Aircraft Configurations in Supersonic Flow. NACA TM 1421, 1957.

3. Whitcomb, Richard T.: A Study of the Zero-Lift Drag-Rise Characteristics of Wing-Body Combinations Near the Speed of Sound. NACA Rep. 1273, 1956. (Supersedes NACA RM L52H08).

4. Whitcomb, Richard T.; and Sevier, John R., Jr.: A Supersonic Area Rule and an Application to the Design of a Wing-Body Combination With High Lift-Drag Ratios. NASA TR R-72, 1960. (Supersedes NACA RM L53H31a).

5. Harris, Roy V., Jr.: An Analysis and Correlation of Aircraft Wave Drag. NASA TM X-947, 1964.

6. Friedrichs, K. O.: Formation and Decay of Shock Waves. Comm. Pure Appl. Math., vol. I, no. 3, Sept. 1948, pp. 211-245.

7. Lighthill, M. J.: The Energy Distribution Behind Decaying Shocks. Phil. Mag., Ser. 7, vol. 41, no. 322, Nov. 1950, pp. 1101-1128.

8. Whitham, G. B.: The Flow Pattern of a Supersonic Projectile. Comm. Pure Appl. Math., vol. 5, no. 3, Aug. 1952, pp. 301-348.

9. Middleton, Wilbur D.; and Carlson, Harry W.: A Numerical Method for Calculating Near-Field Sonic-Boom Pressure Signatures. NASA TN D-3082, 1965.

10. Carlson, Harry W.; Mack, Robert J.; and Morris, Odell A.: A Wind-Tunnel Investigation of the Effect of Body Shape on Sonic-Boom Pressure Distributions. NASA TN D-3106, 1965.

11. Anon: Proceedings of the Sonic Boom Symposium. J. Acoust. Soc. Am., vol. 39, no. 5, pt. 2, May 1966.

12. Seebass, A. R., ed.: Sonic Boom Research. NASA SP-147, 1967.

13. Kuethe, A. M.; and Schetzer, J. D.: Foundations of Aerodynamics. Second ed., John Wiley & Sons, Inc., 1964.

14. Ames Research Staff: Equations, Tables, and Charts for Compressible Flow. NACA Rep. 1135, 1953.

15. Truitt, Robert W.: Hypersonic Aerodynamics. The Ronald Press Co., 1959, p. 225.

NASA-Langley, 1968 — 1 E-4578